

# Attosecond electronic and nuclear quantum photodynamics of ozone: time-dependent Dyson orbitals and dipole

A. Perveaux,<sup>1,2</sup> D. Lauvergnat,<sup>2</sup> B. Lasorne,<sup>1</sup> F.

Gatti<sup>1</sup>, M. A. Robb,<sup>3</sup> G. J. Halász,<sup>4</sup> and Á. Vibók<sup>5</sup>

<sup>1</sup>*CTMM, Institut Charles Gerhardt Montpellier,*

*Université Montpellier 2, F-34095 Montpellier, France*

<sup>2</sup>*Laboratoire de Chimie Physique, Bâtiment 349, CNRS, UMR8000,*

*Orsay, F-91405; Univ Paris-Sud, Orsay, F-91405; France*

<sup>3</sup>*Imperial College London, Department of Chemistry, London SW7 2AZ, UK*

<sup>1</sup>*Department of Information Technology, University of Debrecen,*

*H-4010 Debrecen, PO Box 12, Hungary and*

<sup>4</sup>*Department of Theoretical Physics, University of Debrecen,*

*H-4010 Debrecen, PO Box 5, Hungary\**

A nonadiabatic scheme for the description of the coupled electron and nuclear motions in the ozone molecule was proposed recently (PRA,**88**,023425, (2013)). An initial coherent nonstationary state was prepared as a superposition of the ground state and the excited Hartley band. In this situation neither the electrons nor the nuclei are in a stationary state. The multiconfiguration time dependent Hartree method was used to solve the coupled nuclear quantum dynamics in the framework of the adiabatic separation of the time-dependent Schrödinger equation. The resulting wave packet shows an oscillation of the electron density between the two chemical bonds. As a first step for probing the electronic motion we computed the time-dependent molecular dipole and the Dyson orbitals. The latter play an important role in the explanation of the photoelectron angular distribution. Calculations of the Dyson orbitals are presented both for the time-independent as well as the time-dependent situations. We limited our description of the electronic motion to the Franck-Condon region only due to the localization of the nuclear wave packets around this point during the first 5–6 fs.

## I. INTRODUCTION

In recent years, essential effort has been made to develop different attosecond techniques, see, e.g., [1–3] and further references therein. These techniques are based on an appropriate construction of single ultrashort pulses or trains of such pulses, which allows one to take real-time snapshots of ultrafast transformations of matter. Pump-probe experimental techniques using these ultra short laser pulses [3–8] have made possible to control complex molecular processes. Experimentalists can excite or ionize atoms with a controlled few-cycle laser field and then probe them through the spectrally resolved absorption of an attosecond XUV pulse. It is the simplest experimental technique used to study ultrafast electronic dynamics. During this process one is able to fully image the electronic quantum motion and determine the degree of coherence in the studied system [9–13]. However, the real challenge now is how to transfer this technique to molecules.

Despite the fact that the electron dynamics in molecules almost always are strongly coupled to nuclear dynamics in case of diatomics with only one and two electrons the proper description of the nuclear-electron dynamics is satisfactorily solved. In this case the total time-dependent Schrödinger equations (TDSE) can be solved numerically including both the electronic and nuclear degrees of freedom explicitly [14–24]. Another branch of methods treat the electron dynamics very accurately, while keeping fixed the nuclear geometry. This is a fairly reasonable assumption if the masses of the nuclei are large. In this situation the motion of the electrons takes place due to the pump of a nonstationary electronic state during a period of time that is much shorter than the period of the vibrational motion of the nuclei [25–31]. The really challenging task is to create an electronic wave packet in a neutral few-atom system and then describe precisely its coupled electron nuclear dynamics. Such systems are really large enough not to use the advantage of the solution of the TDSE without separation, but they are not large enough to use the rigid nuclear geometry assumption. In this case the difference between the nuclear vibration period and the period of the motion of the electrons are not always very significant.

Recently, we have investigated the ozone molecule and proposed a new scheme for the description of the coupled electron and nuclear motion [32, 33]. An initial coherent non-

---

\*Electronic address: vibok@phys.unideb.hu

stationary state was prepared by a sub-femtosecond pulse [33]. It is a superposition of the ground state X and the excited weakly-bound state B of the Hartley band [34–37]. In this situation neither the electrons nor the nuclei are in a stationary state, and we used quantum dynamics simulations. The nuclear wave packets, the electronic populations, the relative electronic coherence between the ground X and B electronic states and the electron wave packet dynamics were analyzed. The time evolution of the electronic motion was plotted in the Franck-Condon (FC) region only due to the localization of the nuclear wave packet around this point during the first 5 – 6 fs.

The purpose of this paper is to go further in the photodynamics simulation of this system. We now present the time-dependent dipole moment [38] and investigate the Dyson orbitals [39–43]. While the former one is useful to visualize the exciton migration as the electron density shows a fast oscillation between the two chemical bonds, the Dyson orbitals are known to be central in the explanation of the photoelectron angular distribution. Both the time-independent as well as the time-dependent Dyson orbitals are calculated and their properties are discussed.

In Sec. II. we give a short description of the chosen theoretical approaches. The relevant expressions and formalism will also be presented here. The results and the discussions will be presented in Sec. III. Section IV. provides conclusions.

## II. METHODS AND FORMALISM

The adiabatic partition formalism (beyond Born-Oppenheimer [44]) assumes the total molecular wave function  $\Psi_{tot}(\vec{r}_{el}, \vec{R}, t)$  as a sum of products of electronic wave functions,  $\psi_{el}^k(\vec{r}_{el}; \vec{R})$ , and nuclear wave packets,  $\Psi_{nuc}^k(\vec{R}, t)$ :

$$\Psi_{tot}(\vec{r}_{el}, \vec{R}, t) = \sum_{k=1}^n \Psi_{nuc}^k(\vec{R}, t) \psi_{el}^k(\vec{r}_{el}; \vec{R}). \quad (1)$$

Here  $k$  denotes the  $k$  –  $th$  adiabatic electronic state,  $\vec{r}_{el}$  and  $\vec{R}$  are the electronic and the nuclear coordinates, respectively. We are interested in solving the coupled evolution of the nuclear wave packets,  $\Psi_{nuc}^k(\vec{R}, t)$ , by inserting the product ansatz (1) into the time-dependent Schrödinger equation of the full molecular Hamiltonian. The electronic wave function obeys the time-independent Schrödinger equation for the electronic Hamiltonian  $H_{el}(\vec{R})$

$$H_{el}(\vec{R})\psi_{el}^l(\vec{r}_{el}; \vec{R}) = V_l(\vec{R})\psi_{el}^l(\vec{r}_{el}; \vec{R}), \quad (2)$$

and integrating over the electronic coordinates we can also obtain the coupled nuclear Schrödinger equations:

$$i\hbar \frac{\partial}{\partial t} \Psi_{nuc}^k(\vec{R}, t) = \sum_{l=1, n} H_{k,l}(\vec{R}) \Psi_{nuc}^l(\vec{R}, t). \quad (3)$$

Here  $H_{k,l}$  is the matrix element of the vibronic Hamiltonian, which reads, e.g., for  $n = 2$ ,

$$H = \begin{pmatrix} T_{nuc} + V_k & K_{k,l}^* \\ K_{k,l} & T_{nuc} + V_l \end{pmatrix}, \quad (4)$$

where  $T_{nuc}$  is the nuclear kinetic energy,  $V_k$  ( $k = 1, \dots, n$ ) is the  $k$ -th adiabatic potential energy and  $K_{k,l}$  with  $k \neq l$  is the coupling term between the  $(k, l)$ -th electronic states, which contains the light-matter interaction,  $-\vec{\mu}_{k,l} \cdot \vec{E}(t)$  (electric dipole approximation), where  $\vec{E}(t)$  is an external field resonant between the  $k$ -th and the  $l$ -th states and  $\vec{\mu}_{k,l}$  is the  $\vec{R}$ -dependent transition dipole moment.

One has to solve the electronic and nuclear Schrödinger equations Eqs. (2-3) to obtain the potential energy surfaces and the electronic and nuclear wave functions. The electronic structure calculations are performed by the MOLPRO code [45] and a development version of the GAUSSIAN program package [46]. As for the nuclear dynamics calculations the multiconfiguration time-dependent Hartree method (MCTDH) method [47–50] was used.

The MCTDH nuclear wave packets,  $\Psi_{nuc}^k(\vec{R}, t)$ , contain all the information about the relative phases between the electronic states. Using the interaction picture,  $\Psi_{nuc}^k(\vec{R}, t)$  can equally be written as:

$$\Psi_{nuc}^k(\vec{R}, t) = \exp(-iV_k(\vec{R})t/\hbar) a_k(\vec{R}, t). \quad (5)$$

Here,  $V_k(\vec{R})$  is the potential energy of the  $k$ -th state. The first part of this wave function is the phase factor,  $(\exp(-iV_k(\vec{R})t/\hbar))$ , of the  $k$ -th state, which oscillates very fast.

From the electronic and nuclear wave functions the total density matrix of the molecule, the electronic populations on the different states and the electronic relative coherence between the different electronic states have been calculated [32, 33].

In the present case we have two states (the ground X and the Hartley B states), and the electronic wave packet of the neutral molecule can be written as follows

$$\Psi_{tot}(\vec{r}_{el}, \vec{R}, t) = \Psi_{nuc}^X(\vec{R}, t) \psi_{el}^X(\vec{r}_{el}; \vec{R}) + \Psi_{nuc}^B(\vec{R}, t) \psi_{el}^B(\vec{r}_{el}; \vec{R}). \quad (6)$$

Applying this formula, the total time-dependent dipole of the molecule reads as

$$\vec{\mu}_{tot}(\vec{R}, t) = \left\langle \Psi_{tot}(\vec{R}, t) \mid \vec{\mu}_{tot} \mid \Psi_{tot}(\vec{R}, t) \right\rangle = \sum_{k,l=X,B} \Psi_{nuc}^{k*}(\vec{R}, t) \Psi_{nuc}^l(\vec{R}, t) \vec{\mu}_{k,l}(\vec{R}) \quad (7)$$

here  $\vec{\mu}_{k,l}$  is the transition dipole moment between the  $k$ -th and  $l$ -th electronic states.

Probing the electronic wave packet will lead to ionize the ozone molecule. The Dyson orbitals correspond to the molecular orbitals of the neutral molecule from which an electron has been removed where the cation relaxation is accounted for. They can be computed as one-electron transition amplitudes between the  $N$ -electron neutral and  $(N-1)$ -electron cationic states:

$$\Phi_{cat}^D(\vec{r}; \vec{R}) = \sqrt{N} \int d\vec{r}_1 \dots d\vec{r}_{N-1} \psi_{el,neut}^N(\vec{r}_1, \dots, \vec{r}_N = \vec{r}; \vec{R}) \psi_{el,cat}^{N-1}(\vec{r}_1, \dots, \vec{r}_{N-1}; \vec{R}). \quad (8)$$

Applying the occupation number representation the Dyson orbitals can also be expressed in the molecular orbitals of the neutral molecule

$$\Phi_{cat}^D(\vec{r}; \vec{R}) = \sum_k \varphi_k^{neut}(\vec{r}) \left\langle \psi_{el,cat}^{N-1}(\vec{R}) \mid \hat{a}_k \psi_{el,neut}^N(\vec{R}) \right\rangle. \quad (9)$$

Here  $\hat{a}_k$  is the operator which removes an electron from the molecular orbital  $\varphi_k$ .

We now define the time-dependent Dyson orbitals. These orbitals may be useful for instance when the neutral molecule is excited by an ultrashort laser pulse creating a coherent superposition of the different stationary states in the neutral molecule that will be probed in the next step by sudden XUV ionization. We focus here on such a situation.

$$\begin{aligned} \Phi_{cat,i}^D(\vec{r}; \vec{R}, \tau) &= \sqrt{N} \int d\vec{r}_1 \dots d\vec{r}_{N-1} \psi_{el,neut}^N(\vec{r}_1, \dots, \vec{r}_N = \vec{r}; \vec{R}, \tau) \psi_{el,cat,i}^{N-1}(\vec{r}_1, \dots, \vec{r}_{N-1}; \vec{R}) \\ &= \sum_k \Psi_{nuc}^k(\vec{R}, \tau) \Phi_{cat,i}^D(\vec{r}; \vec{R}), \end{aligned} \quad (10)$$

here  $\tau$  is the time when the ionization takes place.  $i$  denotes the different cation channels. At a given  $\vec{R}$ ,  $\psi_{el,neut}^N(\vec{r}_1, \dots, \vec{r}_N; \vec{R}, \tau)$  is the electronic wave packet, which is a coherent superposition of the ground (X) and the Hartley (B) states, and reads as

$$\psi_{el,neut}^N(\vec{r}_{el}; \vec{R}, \tau) = \Psi_{tot}(\vec{r}_{el}, \vec{R}, \tau) = \Psi_{nuc}^X(\vec{R}, \tau) \psi_{el}^X(\vec{r}_{el}; \vec{R}) + \Psi_{nuc}^B(\vec{R}, \tau) \psi_{el}^B(\vec{r}_{el}; \vec{R}). \quad (11)$$

From this quantity one can form the time-dependent density of the Dyson orbitals at the FC geometry

$$\rho_{\Phi_{cat}^D}(\vec{r}; \vec{R}, \tau) = \sum_{k,l=X,B} \Psi_{nuc}^{k*}(\vec{R}, \tau) \Psi_{nuc}^l(\vec{R}, \tau) \Phi_{cat}^{D,k*}(\vec{r}; \vec{R}) \Phi_{cat}^{D,l}(\vec{r}; \vec{R}). \quad (12)$$

This density can be written for each cation channel as well

$$\begin{aligned} \rho_{\Phi_{cat,i}^D}(\vec{r}; \vec{R}, \tau) = & |\Psi_{nuc}^X(\vec{R}, \tau)|^2 \rho_{\Phi_{cat,i}^{D,X}}(\vec{r}; \vec{R}) + |\Psi_{nuc}^B(\vec{R}, \tau)|^2 \rho_{\Phi_{cat,i}^{D,B}}(\vec{r}; \vec{R}) \\ & + 2Re\Psi_{nuc}^{X*}(\vec{R}, \tau) \Psi_{nuc}^B(\vec{R}, \tau) \Phi_{cat,i}^{D,X*}(\vec{r}; \vec{R}) \Phi_{cat,i}^{D,B}(\vec{r}; \vec{R}) \end{aligned} \quad (13)$$

where index  $i$  runs over each of cation channel.

Let us define the local norm of the Dyson orbitals at the FC geometry, which is approximately proportional to the ionization probability (similar to a Franck-Condon factor in the impulsive picture)

$$\left\langle \Phi_{cat}^D(\vec{r}; \vec{R}, \tau) \mid \Phi_{cat}^D(\vec{r}; \vec{R}, \tau) \right\rangle = \sum_{k,l=X,B} \Psi_{nuc}^{k*}(\vec{R}, \tau) \Psi_{nuc}^l(\vec{R}, \tau) \left\langle \Phi_{cat}^{D,k}(\vec{r}; \vec{R}, \tau) \mid \Phi_{cat}^{D,l}(\vec{r}; \vec{R}, \tau) \right\rangle. \quad (14)$$

For a certain cation channel this quantity reads as:

$$\begin{aligned} \left\langle \Phi_{cat,i}^D(\vec{r}; \vec{R}, \tau) \mid \Phi_{cat,i}^D(\vec{r}; \vec{R}, \tau) \right\rangle = & |\Psi_{nuc}^X(\vec{R}, \tau)|^2 \left\langle \Phi_{cat,i}^{D,X}(\vec{r}; \vec{R}, \tau) \mid \Phi_{cat,i}^{D,X}(\vec{r}; \vec{R}, \tau) \right\rangle \\ & + |\Psi_{nuc}^B(\vec{R}, \tau)|^2 \left\langle \Phi_{cat,i}^{D,B}(\vec{r}; \vec{R}, \tau) \mid \Phi_{cat,i}^{D,B}(\vec{r}; \vec{R}, \tau) \right\rangle \\ & + 2Re\Psi_{nuc}^{X*}(\vec{R}, \tau) \Psi_{nuc}^B(\vec{R}, \tau) \left\langle \Phi_{cat,i}^{D,X*}(\vec{r}; \vec{R}) \mid \Phi_{cat,i}^{D,B}(\vec{r}; \vec{R}) \right\rangle. \end{aligned} \quad (15)$$

These expressions and equations will serve as our working formulae in the next section.

### III. RESULTS AND DISCUSSION

Figure 1 shows the total time-dependent dipole Eq. (7) of the molecule. In the present situation the time-dependent dipole is created after the interaction of the molecule with the

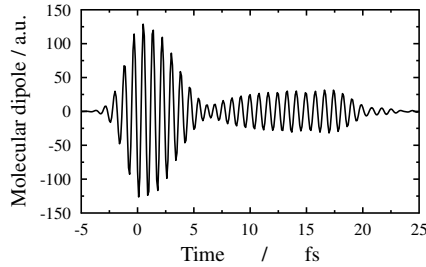


Figure 1: Time-dependent molecular dipole along the y-axis.

Symmetry of the cation state	Excitation energy at the MRCI level [eV]	Experimental value [eV]
${}^2A_1$	12.28	12.73
${}^2B_2$	12.41	13.00
${}^2A_2$	13.09	13.54

Table I: Excitation energies calculated in aug-cc-pvqz basis at the MRCI level of theory for each cation channel. Experimental excitation energies are also presented [51].

pump laser field [38]. Its oscillatory behaviour can be considered as a direct consequence of the coherent superposition of the X and B electronic states. This quantity has a similar time evolution to the electronic relative coherence, which illustrates exciton migration. The FC point of the ozone molecule has  $C_{2v}$  symmetry and therefore only the  $y$ -component ( $B_2$ ) of the transition dipole between the ground state X ( ${}^1A_1$ ) and Hartley B ( ${}^1B_2$ ) is nonzero. The only effective polarization of the electric field is  $y$ .

Probing the electronic wave packet Eq. (11) will lead to ionize the neutral molecule. We focus here on the ionization threshold of the spectrum (fastest electrons). The three lowest cationic states ( ${}^2A_1$ ,  ${}^2B_2$ , and  ${}^2A_2$ ) must be considered together because they are energetically close with respect to the expected bandwidth of the probe pulse. We have calculated the energies of the different electronic states of the cation at the MRCI level of theory and compared them to the experimental values [51]. Reasonably good agreement has been obtained for each electronic state. Results are presented in Table 1.

We now present the Dyson orbitals. They are very illustrative as they are one-electron wave functions that represent the probability amplitude of the electron that is removed from the neutral molecule. They also play an important role in the interpretation of the photoelectron angular distribution as well. Namely, they are approximately proportional

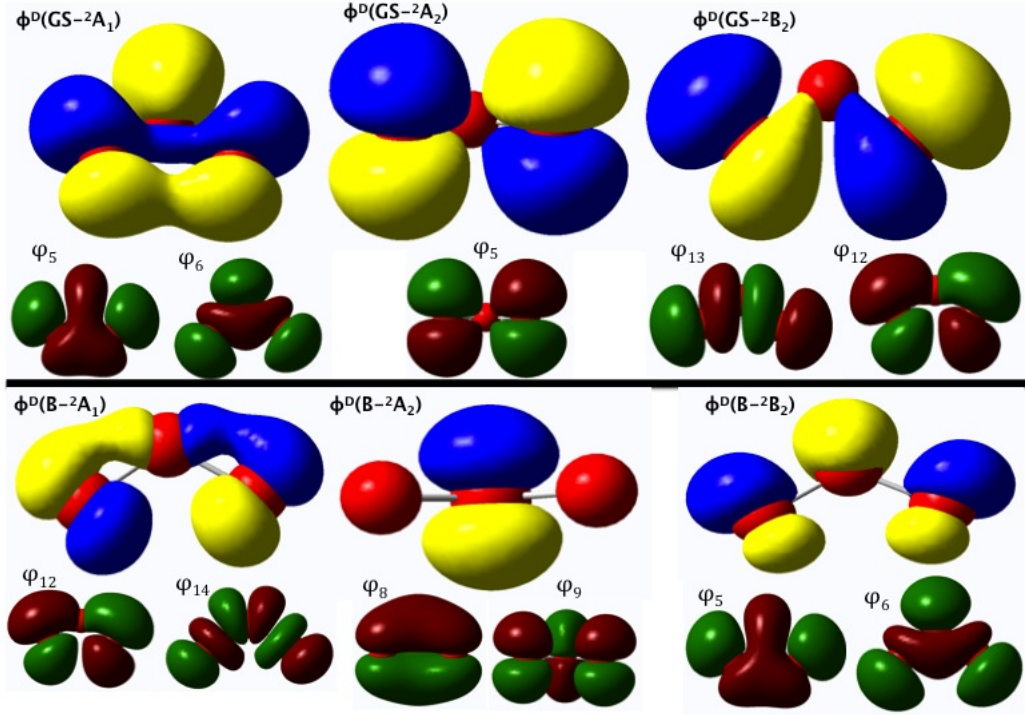


Figure 2: Time-independent Dyson orbitals between the two different electronic states (X, B) of the neutral and the three different channels ( $^2A_1$ ,  $^2B_2$  and  $^2A_2$ ) of the cation. The most important molecular orbital components of the Dyson orbitals are also shown.

to the latter, as their norms give some contributions to the photoionization intensity. In the present situation we have three ionization channels for the ground (X) and also for the Hartley (B) states of the neutral molecule. These six different time-independent Dyson orbitals are calculated according to Eqs. (8 - 9) and are shown in Figure 2. The MRCI method with aug-cc-pvqz basis set was used in the numerical simulations.

As already discussed the Dyson orbitals can also be written as linear combinations of the molecular orbitals of the neutral molecule Eq. (8). As it can be seen in Fig. 2 they follow the Koopman's like rule. Hence, the Dyson orbitals for each cation channel are constructed mainly from one or two neutral's orbitals. Below we give the most important molecular orbitals contributions to the different type of time-independent Dyson orbitals calculated for the present situation:



$$\begin{aligned}
({}^2A_1)\Phi_{X-{}^2A_1}^D &= -0.61\varphi_5 + 0.45\varphi_6; \\
({}^2A_2)\Phi_{X-{}^2A_2}^D &= -0.79\varphi_{15}; \\
({}^2B_2)\Phi_{X-{}^2B_2}^D &= 0.62\varphi_{12} - 0.24\varphi_{13}; \\
({}^2B_2)\Phi_{B-{}^2A_1}^D &= -0.22\varphi_{12} - 0.062\varphi_{14}; \\
({}^2B_1)\Phi_{B-{}^2A_2}^D &= 0.16\varphi_8 - 0.073\varphi_9; \\
({}^2A_1)\Phi_{B-{}^2B_2}^D &= -0.24\varphi_5 + 0.0993\varphi_6.
\end{aligned} \tag{16}$$

The symmetries of the Dyson orbitals are provided by the symmetries of the cation states and the symmetries of the X and B states of the neutral.

Our initial wave function of the neutral ozone molecule is a wave packet, Eq. (6), which is a superposition of two electronic states (X and B). Therefore, the Dyson orbitals are the superpositions of Dyson orbitals from each electronic states of the neutral to the cation. Thus, we are going to have three time-dependent Dyson orbitals Eq. (10); one for each cation channel ( ${}^2A_1$ ,  ${}^2B_2$  and  ${}^2A_2$ ).

In Figures (3-5) the time-dependent densities of the Dyson orbitals are presented. They are calculated according to Eqs. (10,12,13). It can be noticed that the time-dependent densities of the Dyson orbitals are quite similar to the graphical representation of the time-independent Dyson orbitals between the X state of the neutral and an appropriate electronic state of the cation. This is due to the fact that the population on the ground state is always more pronounced than in the excited state (in our case it is the Hartley (B) band). The time-dependent densities of the Dyson orbitals oscillate in time with the same period as the dipole moment of the neutral wave packet which is the period of the coherence. Therefore, there are three different stages in the time evolution of the time-dependent densities of the Dyson orbitals. The first period is between  $[-5.5 ; 6]$  fs when the laser light is on and there is significant relative electronic coherence between the X and B states. In the second period  $[5.5 ; 8]$  fs the laser pulse is off and there is no coherence between the different electronic states. Finally, the third period is  $[9 ; 20]$  fs when the pump pulse is still off but the electronic coherence reappears between the ground X and the Hartley B states of the ozone molecule. The oscillations of the time-dependent densities are the most pronounced in the first interval as the relative electronic coherence is the most significant here. In the

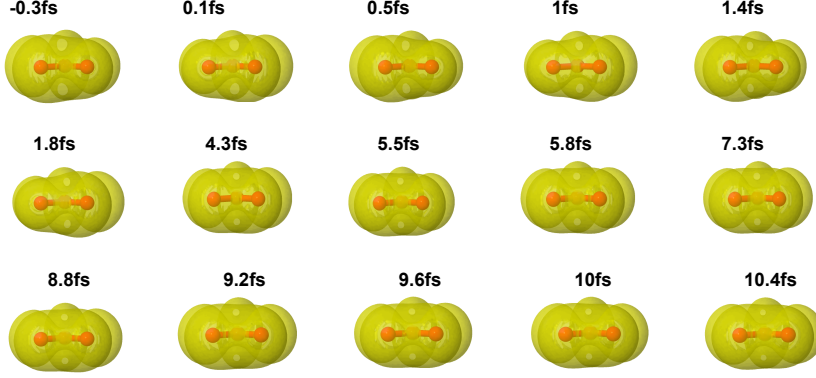


Figure 3: Time-dependent densities of the Dyson orbitals belong to  $^2A_1$  cation channel.

second region there is practically no motion of the time-dependent densities due to a lack of coherence. As for the third stage, the revival of electronic coherence induces a revival of motion in the time-dependent densities but with much less amplitude than the first interval. The latter is due to the fact that the coherence in the field free situation is less prominent than in presence of the light field. Although all three regions were properly included in the numerical simulations the time evolution of the time-dependent densities in the snapshots (Figs. (3-5)) are only presented between the period of  $[-0.3 ; 10.4]$  fs.

We have also calculated the local norms of the Dyson orbitals Eqs. (14,15). These quantities are approximately proportional to the ionization probabilities. Probability densities at the FC geometry, are shown in Figure 6. They can be considered as "local norms", or rather local weights, with values higher than 1. At first sight, the striking feature on the pictures (see Figs. 6a - 6b) is that the ground X state is the essential component of the Dyson orbital's norm. This is consistent with the previous finding that the population in the ground X state is more pronounced than that one on the Hartley B state. We can also notice, that the cation channel that presents more coherence ( $^2B_2$ ) is at the same time the one that provides less total probability. And the reverse is also true, namely that the one presenting less coherence ( $^2A_2$ ) is the one presenting more total probability. It is partly explained by the fact that the more there is population on the ground X state, the less there is on the Hartley B state, therefore the less there is electronic coherence between these two (neutral and cation) excited states (see Fig. 6c). On the other hand the more there is population on the ground X state the more the probability of the time-dependent Dyson

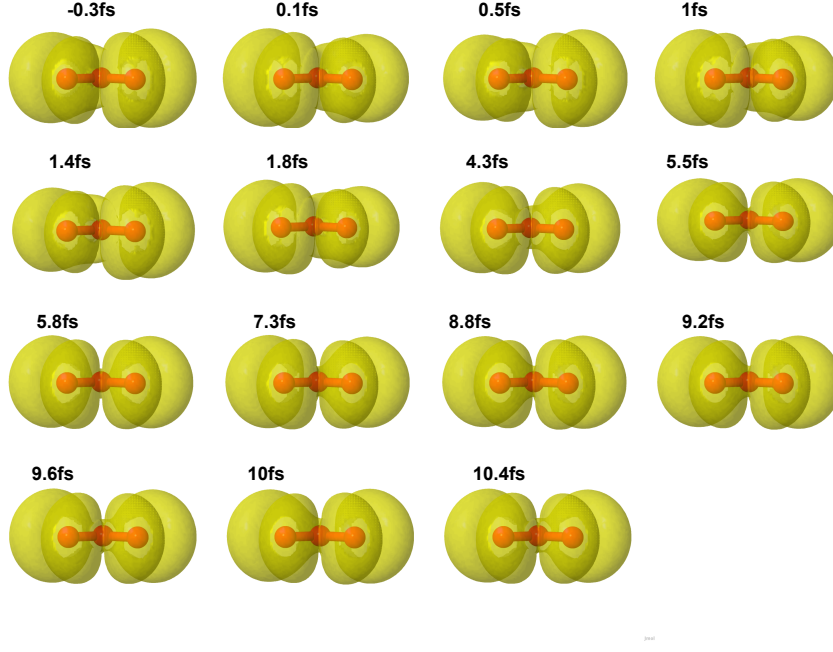


Figure 4: Time-dependent densities of the Dyson orbitals belong to  $^2B_2$  cation channel.

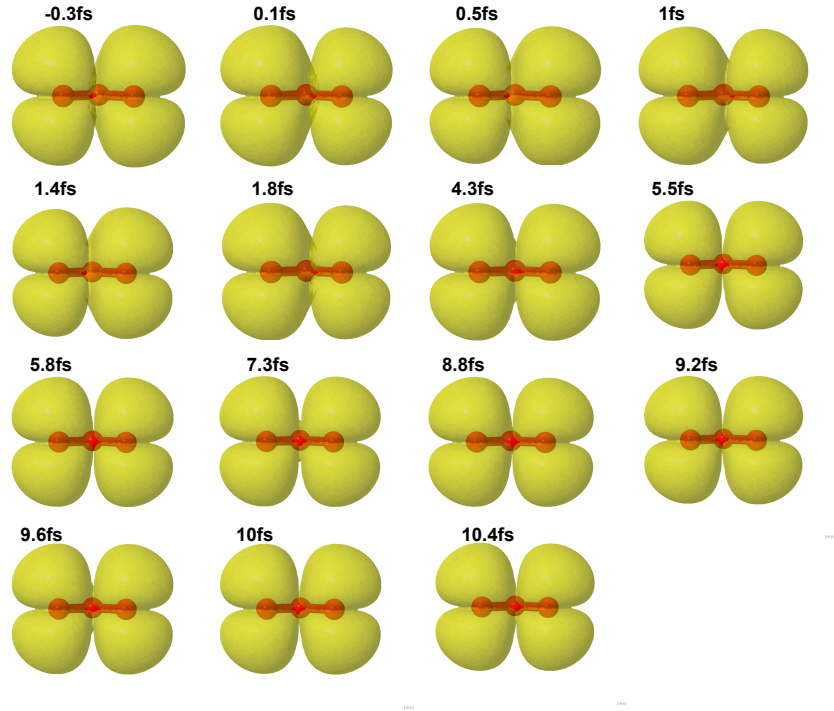


Figure 5: Time-dependent densities of the Dyson orbitals belong to  $^2A_2$  cation channel.

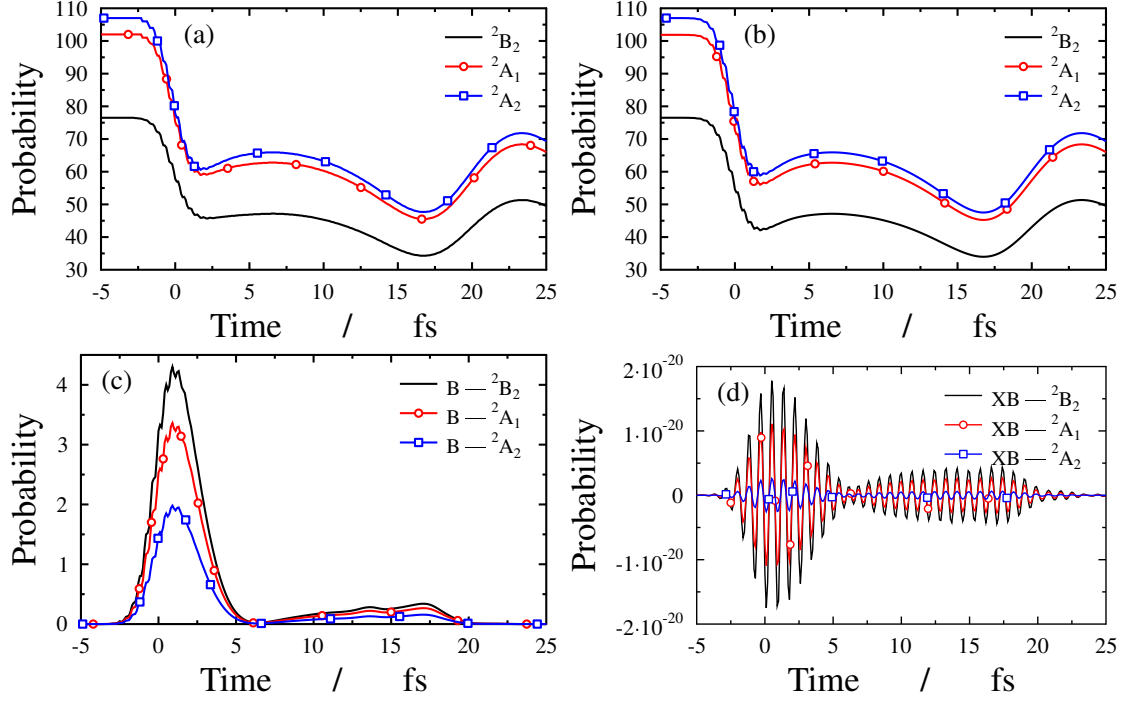


Figure 6: Probability density of the time-dependent Dyson orbitals between the different states of the neutral molecule and the cation as a function of time [fs]. (a): Total probability density of the time-dependent Dyson orbitals as a function of time;  ${}^2B_2$  channel (unmarked);  ${}^2A_2$  channel (marked with square);  ${}^2A_1$  channel (marked with circle). The total probability density can be obtained as a sum of the probability densities on sub figures (b) and (c). (b): Probability density of the time-dependent Dyson orbitals as a function of time between the X state of the neutral and the different states of the cation;  ${}^2B_2$  channel (unmarked),  ${}^2A_2$  channel (marked with square);  ${}^2A_1$  channel (marked with circle). (c): Probability density of the time-dependent Dyson orbitals as a function of time between the B state of the neutral and the different states of the cation;  ${}^2B_2$  channel (unmarked),  ${}^2A_2$  channel (marked with square);  ${}^2A_1$  channel (marked with circle). (d): Probability density of the relative electronic coherence of the X and B states of the neutral with the  ${}^2B_2$  cation channel (unmarked),  ${}^2A_2$  cation channel (marked with square);  ${}^2A_1$  cation channel (marked with circle) as a function of time.

orbitals increases.

#### IV. CONCLUSIONS

We have started to develop a complex theoretical description of the coupled electron and nuclear motion in the ozone molecule on the attosecond time scale [32, 33]. An initial coherent nonstationary state was created as a coherent superposition of the ground X and excited Hartley B states. In this situation we were able to induce attosecond electron dynamics in the neutral molecule. The MCTDH approach was used to solve the dynamical Schrödinger equation for the nuclei in the framework of the time-dependent adiabatic partition including the light-matter interaction (electric dipole approximation). Based on this dynamical simulation the description of the time evolution of the electronic motion is limited only to the Franck-Condon region due to the localization of the nuclear wave packet around this point during the first 5 – 6 fs.

Applying the nuclear wave packet we have determined the total density matrix of the molecule and from it were able to calculate the electronic populations and the relative electronic coherence between the ground X and B electronic states [33]. In order to calculate the excited-state differential charge density at the FC point we used the total molecular wave packet which is a coherent mixture of multiple electronic states, whereby the time-dependent coefficients are the nuclear wave packets. As a results, an oscillation of the electronic cloud between the two chemical bonds was observed with a 0.8 fs period of time [33].

Going further in our photodynamics description we calculated the time-dependent dipole moment and the Dyson orbitals. They are very useful to visualize the exciton migration within the molecule as the electron density oscillates between the two chemical bonds. In addition, the Dyson orbitals are known to be important in the explanation of the photoelectron angular distribution. We calculated both the time-independent as well as the time-dependent Dyson orbitals and discussed their properties for different situations. Corresponding experiments are in progress [52].

#### Acknowledgements

The authors would like to thank R. Kienberger , M. Jobst and F. Krausz, for support and for fruitful discussions. We acknowledge R. Schinke for providing the potential energy surfaces and the transition dipole moment and H.-D. Meyer for fruitful discussions. The au-

thors also acknowledge the TÁMOP 4.2.4. A/2-11-1-2012-0001 project. Á.V. acknowledges the OTKA (NN103251). Financial support by the CNRS-MTA is greatly acknowledged.

- 
- [1] Corkum P B and Krausz F 2007 *Nature Phys.* **3** 381
  - [2] Goulielmakis E, et. al. 2008 *Science* **320** 1614
  - [3] Krausz F and Ivanov M 2009 *Rev. Mod. Phys.* **81** 163
  - [4] Smirnova O, Mairesse Y, Patchkovskii S, Dudovich N, Villeneuve D, Corkum P and Ivanov M Y *Nature* **460** 972
  - [5] Huismans Y, et al. 2011 *Science* **331** 61
  - [6] Kapteyn H C and Murnane M 2010 XXII International Conference on Raman Spectroscopy **92** 39
  - [7] Singh K P, et al. 2010 *Phys. Rev. Lett.* **104** 023001
  - [8] Zhou X, Ranitovic P, Hogle C W, Eland J H D, Kapteyn H C and Murnane M M 2012 *Nat. Phys.* **8** 232
  - [9] Rohringer N, Gordon A and Santra R 2006 *Phys. Rev. A* **74** 043420
  - [10] Rohringer N and Santra R 2009 *Phys. Rev. A* **79** 053402
  - [11] Kelkensberg F, et al. 2009 *Phys. Rev. Lett.* **103** 123005
  - [12] Goulielmakis E, et. al. 2010 *Nature Lett.* **466** 739
  - [13] Dixit G, Vendrell O and Santra R 2012 *PNAS* **109** 11636
  - [14] Bandrauk A D, Chelkowski S and Nguyen H S 2004 *Int. J. Quant. Chem.* **100** 834
  - [15] Bandrauk A D, Chelkowski S, Corkum P B, Manz J and Yudin G L 2009 *J. Phys. B:* **42** 134001
  - [16] Kelkensberg F, Siu W, Perez-Torres J F, et. al. 2011 *Phys. Rev. Lett.* **107** 043002
  - [17] Fischer B, Pfeifer M T, et. al. 2010 *Phys. Rev. Lett.* **105** 223001
  - [18] Pérez-Torres J F, Morales F, Sanz-Vicario J L and Martín F 2009 *Phys. Rev. A* **80** 011402
  - [19] Sansone G, Kelkensberg F, Pérez-Torres J F, et. al. 2010 *Nature* **465** 763
  - [20] Grafe S, Engel V and Ivanov M Y 2008 *Phys. Rev. Lett.* **101** 103001
  - [21] Geppert D, von den Hoff P and de Vivie-Riedle R 2008 *J. Phys. B:* **41** 074006
  - [22] von den Hoff P, Znakovskaya I, Kling M F and de Vivie-Riedle R 2009 *Chem. Phys.* **366** 139
  - [23] Znakovskaya I, von den Hoff P, Zhrebtsov S, Wirth A, Herrwerth O, Vrakking M J J, de Vivie-Riedle R and Kling M F 2009 *Phys. Rev. Lett.* **103** 103002

- [24] von den Hoff P, Siemering R, Kowalewski M and de Vivie-Riedle R 2012 IEEE Journal of Selected Topic in Quantum Electronics, **18** 1
- [25] Remacle F, Kienberger R, Krausz F and Levine R D 2007 Chem. Phys. **338** 342
- [26] Remacle F and Levine R D 2007 Z. Phys. Chem. **221** 647
- [27] Remacle F, Nest M and Levine R D 2007 Phys. Rev. Lett. **99** 183902
- [28] Muskatel B H, Remacle F and Levine R D 2009 Phys. Scr. **80** 048101
- [29] Remacle F and Levine R D 2011 Phys. Rev. A **83** 013411
- [30] Mignolet B, Levine R D and Remacle F 2012 Phys. Rev. A **86** 053429
- [31] Nest M 2009 Chem. Phys. Lett. **472** 171
- [32] Halász G J, Perveaux A, Lasorne B, Robb M A, Gatti F and Vibók Á 2012 Phys. Rev. A **86** 043426
- [33] Halász G J, Perveaux A, Lasorne B, Robb M A, Gatti F and Vibók Á 2013 Phys. Rev. A **88** 023425
- [34] Qu Z W, Zhu H, Grebenshchikov S Yu and Schinke R 2005 J. Chem. Phys. **123** 074305
- [35] Baloitcha E and Balint-Kurti G G 2005 J. Chem. Phys. **123** 014306
- [36] Grebenshchikov S Yu, Qu Z W, Zhu H and Schinke R 2007 Phys. Chem. Chem Phys. **9** 2044
- [37] Schinke R and McBane G C 2010 J. Chem. Phys. **132** 044305
- [38] Neidel C, et. al. 2013 Phys. Rev. Lett. **111** 033001
- [39] Mignolet B, Kus T and Remacle F 2013 Imaging and Manipulating Molecular Orbitals Advances in Atom and Single Molecule Machines pp 41-54.
- [40] Oana C M and Krylov A I 2007 J. Chem. Phys. **127** 234106
- [41] Oana C M and Krylov A I 2009 J. Chem. Phys. **131** 124114
- [42] Spanner M and Patchkovskii S 2009 Phys. Rev. A **80** 063411
- [43] Spanner M, et. al. 2012 Phys. Rev. A **86** 053406
- [44] Baer M 2006 Beyond Born Oppenheimer: Electronic Non-Adiabatic Coupling Terms and Conical Intersections; Wiley: Hoboken, NJ
- [45] MOLPRO, version 2006,1, a package of ab initio programs, H.-J. Werner, P.J. Knowles, R. Lindth, et al., see [http:// www.molpro.net](http://www.molpro.net).
- [46] Frisch M J, et. al. 2009 Gaussian Dev. Version, Revision H.01 (Gaussian, Inc., Wallingford CT)
- [47] Meyer H D, Manthe U and Cederbaum L S 1990 Chem. Phys. Lett. **165** 73

- [48] Manthe U, Meyer H D and Cederbaum L S 1992 J. Chem. Phys. **97** 3199
- [49] Beck M H, Jäckle A, Worth G A and Meyer H D, 2000 Phys. Rep. **324** 1; Worth G A et. al. 2000 The MCTDH Package, Version 8.2, 2002 Version 8.3, 2007Version 8.4, University of Heidelberg, Germany; See <http://mctdh.uni-hd.de/>.
- [50] Meyer H D, Gatti F and Worth G A 2009 Eds.; Multidimensional Quantum Dynamics: MCTDH Theory and Applications. Wiley-VCH, Weinheim
- [51] Katsumata S, Shiromaru H and Kimura T 1984 Bull. Chem. Soc. Jpn. **57** 1784
- [52] Kienberger R, Jobst M and Krausz F Private Communication.